Oxidation of Tryptamine and 5-Hydroxytryptamine: A Pulse Radiolysis and Quantum Chemical Study

P. Gaikwad,[†] K. I. Priyadarsini,[‡] S. Naumov,[§] and B. S. M. Rao*[,†]

National Centre for Free Radical Research, Department of Chemistry, University of Pune, Pune-411 007, India, Radiation & Photochemistry Division, Bhabha Atomic Research Centre, Trombay, Mumbai-400 085, India, and Leibniz-Institut für Oberflächenmodifizierung e.V. (IOM), Permoser Strasse 15, D-04318 Leipzig, Germany

Received: February 12, 2009; Revised Manuscript Received: June 9, 2009

The reactions of oxidizing radicals $^{\bullet}OH$, $N_3^{\bullet}$, $Br_2^{\bullet-}$, and $NO_2^{\bullet}$ with tryptamine (Tpe) and 5-hydroxytryptamine (HTpe) were studied by pulse radiolysis and analyzed by quantum chemical calculations. Barring $NO_2^{\bullet}$ radical, the rate constants for their reaction with Tpe and HTpe were found to be diffusion controlled and the rates in the $NO_2^{\bullet}$ radical reaction with HTpe are lower by 2 orders of magnitude with $k \sim 1 \times 10^7$ dm^3 mol^{-1} s^{-1}. The transient spectra formed on oxidation of Tpe and HTpe exhibited peaks at 330 and 530 nm (indolyl radical) and 420 nm (indoloxyl radical), respectively, and the latter is in reasonable agreement with the calculated value (407 nm). Both radicals decay through direct recombination, but only the indoloxyl radical was observed to react with the parent molecule to give a (HTpe−Ind)$^{\bullet}$ radical adduct for [HTpe] $\geq 50 \times 10^{-6}$ mol dm^{-3}. The calculated optimized geometries in water revealed the formation of two distinct types of radical adducts, one through the H−O bond and the other by C−C linkage. The H−O bonded radical adduct was found to be exothermic with a reaction enthalpy of −4 kcal mol^{-1} and bond length 0.1819 nm and the C−C bonded radical adducts are endothermic and rate determining but are finally driven by exothermic processes involving intermolecular H transfer followed by intramolecular reorganization through H shift resulting in stable C4−C4′ and C2−C4′ dimers with reaction enthalpies of −39 and −44 kcal mol^{-1}, respectively, and this process was found to be thermodynamically as efficient as direct recombination of indoloxyl radicals. The formation of the two dimer products was also seen in steady-state radiolysis. The lack of adduct formation in the case of indolyl radical with Tpe is due to the positive free energy change ($\Delta G = 10$ kcal mol^{-1}). The energetics for the $^{\bullet}OH$ addition have shown dependence on the site of activation with (HTpe−OH)$^{\bullet}$ adducts at C2 and C4 and the (Tpe−OH)$^{\bullet}$ adduct at C2 being more thermodynamically stable and the water elimination to give the indoloxyl radical proceeds fast from (HTpe−OH)$^{\bullet}$ adduct at C4 due to favorable geometry.

Introduction

5-Hydroxytryptamine, also well-known as serotonin, is an important biomolecule that is found in significant amounts in the central nervous system.[1–3] The analysis of HTpe in various regions of mammalian brain revealed concentrations ranging from (0.7 to 42) $\times 10^{-6}$ mol dm^{-3} in wet tissue, but much higher concentrations are usually present in central and peripheral nervous systems.[3] The free radical induced oxidative modification of serotonin—forming toxic dihydroxylated dimer products—is implicated in neurodegenerative diseases.[3,4] Thus, anomalous oxidation of serotonin is reported[4] to cause Alzheimer and Parkinsonism diseases. The oxidation of serotonin and other 5-hydroxyindoles has been studied[5–14] earlier by radiation chemical and other methods. Of particular mention are the studies on electrochemical oxidation of indoles by Dryhurst and co-workers.[3]

$NO_2^{\bullet}$ is an important radical[15] in biology and can be conveniently generated by pulse radiolysis using N_2O saturated aqueous solutions containing buffered sodium nitrite or N_2-saturated solution of a mixture of nitrite and nitrate. It can undergo several reactions such as recombination with radical species, addition to double bonds, electron transfer, and hydrogen abstraction from C−H bonds of unsaturated compounds.[16,17] It is interesting to investigate the reactions of $NO_2^{\bullet}$ radical with serotonin as it was not studied earlier.

In the one-electron oxidation by $Br_2^{\bullet-}$ radical of 5-hydroxytryptophol and tryptophol, it has been shown[14] that the indoloxyl radical adds to 5-hydroxytryptophol whereas no such reaction was seen in the case of tryptophol. It was further shown that [5-hydroxytrptophol] as low as 5×10^{-5} mol dm^{-3} resulted in the dimerization. On the basis of theoretical calculations in the gas phase, the authors proposed that the reaction occurs through the C−C linkage from interaction of 5-hydroxytryptophol and the indoloxyl radical. Furthermore, on the basis of semiempirical methods at the ZINDO level of theory on PM3 optimized geometry, their excited state calculations in the gas phase for the above three transients have shown absorption maxima at 370−380 nm and the other three possible stable conformers for O−C linked radical adducts were predicted to absorb at ∼300 nm with small oscillator strengths ($f \sim 0.02$). The product distribution of HTpe on electrochemical oxidation is affected by secondary reactions in contrast to the radiation-induced oxidation which is selective. Radiation chemistry can, thus, provide valuable information on kinetics, transient spectra, and the reaction mechanism.

* Corresponding author. E-mail: bsmr@chem.unipune.ernet.in. Fax: 0091-20-25691728. Ph: 0091-20-25601141.
[†] University of Pune.
[‡] Bhabha Atomic Research Centre.
[§] Leibniz-Institut für Oberflächenmodifizierung e.V.

10.1021/jp901315q CCC: $40.75
Published on Web 07/01/2009

There is, therefore, a need for a detailed investigation to ascertain the nature of bonding of the radical adduct and subsequent chemical reactions occurring in indole derivatives. In this work, two model compounds, tryptamine (Tpe) and 5-hydroxytrptamine (HTpe) (see Scheme 1 for structures) have been chosen to study their oxidation by $^{\bullet}OH$, $N_3^{\bullet}$, $Br_2^{\bullet-}$, and $NO_2^{\bullet}$ radicals by pulse radiolysis and quantum chemical methods using B3LYP/6-31+G(d,p) level of theory. A few experiments on product analysis by HPLC were also carried out. This paper will particularly address the following: why does the radical adduct formation occur only with the indoloxyl radical and not with the indolyl radical, what is the mechanism for the formation of toxic dimer products, how efficient are these processes thermodynamically, which reductants are effective for the repair of indoloxyl radical, and finally what are the relative stabilities of isomeric $(HTpe-OH)^{\bullet}$ adducts toward the formation of indoloxyl radical by dehydration.

Experimental Section

Chemicals. Tpe, HTpe, and $ABTS^{2-}$ (2,2-azino-bis-3-ethylbenzothiazoline-6-sulfonate) from Sigma and MV^{2+} (methyl viologen) from Aldrich were obtained and used as received. All other chemicals and N_2/N_2O gases used were of high grade purity. Solutions were prepared with water purified by a Millipore Milli-Q system, and freshly prepared solutions were used for each experiment. pH was adjusted with $NaOH/HClO_4$ or the phosphate buffer.

Irradiations. Pulse radiolysis studies were performed with high-energy electron pulses (7 MeV, 50 ns) at the National Centre for Free Radical Research, University of Pune, Pune[18,19] coupled to an optical detection system. The dose delivered per pulse was determined by thiocyanate dosimtery.[20] The dose per pulse was in general kept between 8 and 12 Gy. Pulse radiolysis experiments were carried out in Suprasil cuvettes with a cross-sectional area of 1 cm^2 at 25 °C. Radiolysis of water (reaction 1) produces three highly reactive species ($^{\bullet}OH$, $^{\bullet}H$, e^-_{aq}) in addition to the formation of less reactive or inert molecular species (H_2, H_2O_2, H_3O^+). The hydrated electron (e^-_{aq}) reacts with N_2O and is converted into hydroxyl radical (reaction 2). N_2O saturated aqueous solutions containing 2×10^{-2} mol dm^{-3} nitrite were pulse radiolysed to produce $NO_2^{\bullet}$ radical (reaction 3).

In aqueous solutions, the $NO_2^{\bullet}$ radical exists in equilibrium with its dimer, dinitrogen tetroxide (N_2O_4) (reaction 4). Dimerization is fast in aqueous solutions ($k = 4.5 \times 10^8$ dm^3 $mol^{-1}s^{-1}$) and the solubility of the dimer in water is about 100 times higher than that of nitrogen dioxide.[21,22] Once formed N_2O_4 decays by a relatively fast reaction with water to produce nitrite and nitrate (reaction 5).[15,23,24]

$$H_2O \rightarrow {}^{\bullet}OH,\ {}^{\bullet}H,\ e^-_{aq},\ H_2,\ H_2O_2,\ H_3O^+ \quad (1)$$

$$e^-_{aq} + N_2O \rightarrow N_2 + OH^- + {}^{\bullet}OH \quad (2)$$

$$NO_2^- + {}^{\bullet}OH \rightarrow NO_2^{\bullet} + OH^- \quad (3)$$

$$NO_2^{\bullet} + NO_2^{\bullet} \rightarrow N_2O_4 \quad (4)$$

$$N_2O_4 + H_2O \rightarrow NO_3^- + NO_2^- + 2H^+ \quad (5)$$

The one-electron oxidants, $N_3^{\bullet}$ and $Br_2^{\bullet-}$ radicals, were generated by radiolysis of N_2O saturated aqueous solutions containing 5×10^{-2} mol dm^{-3} NaN_3 and 0.1 mol dm^{-3} KBr, respectively.[11,13,14]

HPLC Analysis. The Shimadzu HPLC system (Prominence 20A) and a RP-18 column (25 cm × 0.45 cm) were used. Two different protocols were used. The protocol 1 consisted of H_2O/MeOH (35:65 v/v) (flow rate 1 mL min^{-1}). Protocol 2 is identical to that reported earlier[25,26] in electrochemical oxidation consisting of 3 mL of 25% ammonia and H_2O/MeCN (100:7 v/v, solvent A) and (100:40 v/v, solvent B) at pH 3.5. The measurements were done with 100% solvent A during 0−30 and 30−55 min but with flow rates of 0.35 and 1.25 mL min^{-1}, respectively, and 100% solvent B for the last 5 min (55−60 min) with a flow rate 1.5 mL min^{-1}. The eluent was monitored at 275 nm in both cases.

Theoretical Studies. Density functional theory (DFT) calculations were carried out using Becke's three-parameter functional (B3)[27,28] in combination with the Lee, Yang, and Parr (LYP) correlation functional.[29] The molecular geometries, energies, and frequency analysis were calculated both in the gas phase and in water at the same B3LYP/6-31+G** (Jaguar version 7.0 program[30]) level of theory. The solvent correction was applied using the UB3LYP/6-311+G(d,p)/SCRF=CPCM method and was analyzed using Jaguar's dielectric continuum Poisson−Boltzmann solver, which fits the field produced by the solvent dielectric continuum to another set of point charges.[31] The frequency analysis was made on the structures optimized in gas phase to obtain thermodynamic parameters such as zero point energy (ZPE), entropy (S), and Gibbs free energy (ΔG) at 298 K. The electronic transition spectra were calculated using the unrestricted time dependent (UTD)[32] B3LYP/6-31+G(d,p) method as implemented in Gaussian 03 program.[33]

Results and Discussion

Kinetics and Spectra. ***Tpe.*** The rates of the reaction of $^{\bullet}OH$ radical with Tpe were determined by monitoring the growth at

SCHEME 1: The Reaction Sequence for the $^{\bullet}OH$ Radical Addition (Reaction 1) to HTpe and Tpe and for the Water Elimination (Reaction 2)

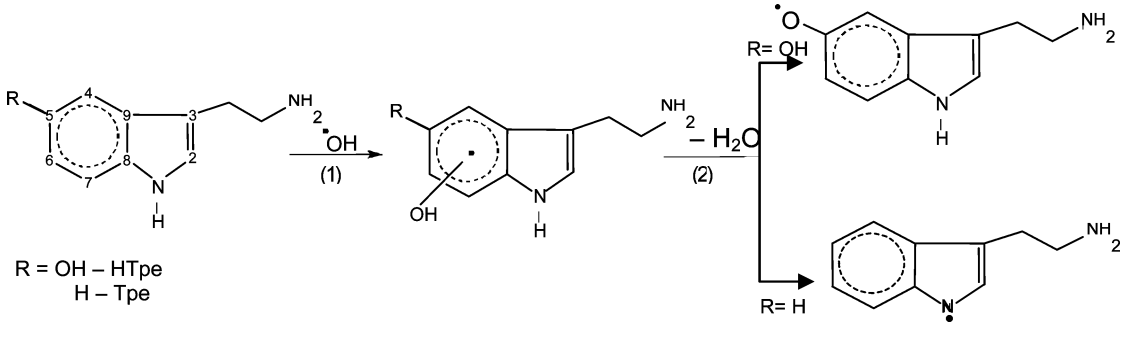

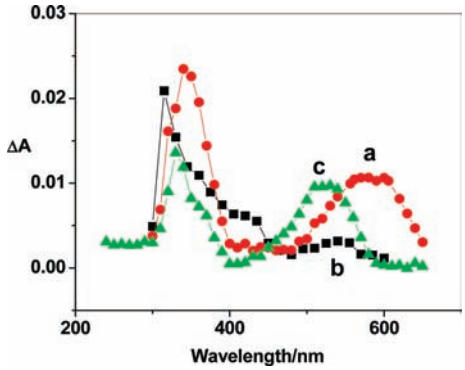

Figure 1. Transient absorption spectra obtained at 40 μs after pulse in the reactions of $^{\bullet}$OH (a and b) and $N_3^{\bullet}$ (c) radicals with 1×10^{-3} mol dm^{-3} Tpe under different solution conditions: (a) aerated at pH 1 and (b) N_2O saturated solutions at pH 7; (c) N_2O saturated solution containing 5×10^{-2} mol dm^{-3} NaN_3 at pH 7. The intensities of spectrum a were doubled to normalize with spectra b and c. Dose per pulse = 8 Gy.

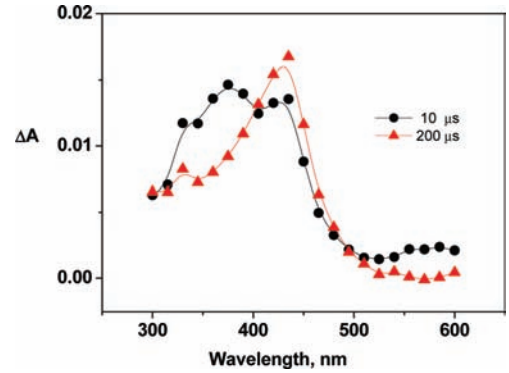

Figure 2. Transient absorption spectra obtained on reaction of $^{\bullet}$OH radical with HTpe (1×10^{-3} mol dm^{-3}) at pH 5. Dose per pulse = 8 Gy.

the absorption maxima (315−330 nm), and the pseudo-first-order rate constants were found to be linearly dependent in the concentration range $(0.5-2.5) \times 10^{-4}$ mol dm^{-3}. The measured rate constants in buffered solutions (pH 7) were found to be nearly diffusion-controlled with $k = 8.6 \times 10^9$ dm^3 mol^{-1} s^{-1}. The values remained unaffected in the pH 5−9 with $k = (6-8) \times 10^9$ dm^3 mol^{-1} s^{-1}. With the $N_3^{\bullet}$ radical, the rate constant measured with Tpe at pH 7 is 3.6×10^9 dm^3 mol^{-1}s^{-1}, which is similar to that measured in acidic and basic media.

Figure 1 depicts the transient absorption spectra measured in the reaction of $^{\bullet}$OH and $^{\bullet}N_3$ radicals with Tpe at pH 1 and 7. The reaction at pH 1 was carried out using $HClO_4$ in aerated solutions containing Tpe (1×10^{-3} mol dm^{-3}), where the $^{\bullet}$OH radical ($G = 2.8$ per 100 eV) reacts with Tpe and the H atom with oxygen (reactions 6 and 7).

$$e^-_{aq} + H^+ \rightarrow H \quad (6)$$

$$H + O_2 \rightarrow HO_2 \quad (7)$$

The spectrum measured in the $N_3^{\bullet}$ radical reaction with Tpe in neutral solution (Figure 1) at 40 μs has two distinct peaks at 330 and 530 nm, with the former having higher intensity. No differences in the spectral features were seen in the range pH 5−9. The spectrum recorded by us in the reaction of $Br_2^{\bullet-}$ with Tpe in neutral solutions (not shown) is similar to that measured in $N_3^{\bullet}$ radical reaction. Though the features in the spectrum of indolyl radical reported by Hela et al.[6] are the same, it has slightly higher intensity at the longer wavelength but all our spectra are identical to those reported on radiation-induced oxidation of tryptophol[14] and 5,6-dimethoxyindole.[8b] The extinction coefficients estimated from our spectra for the indolyl radical in neutral solutions are $\varepsilon_{330} = 3300$ and $\varepsilon_{530} = 2400$ dm^3 mol^{-1}cm^{-1}.

The absorbance values obtained in the $^{\bullet}$OH radical reaction with tryptamine at pH 1 (Figure 1) were doubled to normalize with those measured in N_2O saturated solutions. It can be seen that the spectrum recorded at 40 μs in acidic medium has two distinct peaks at 340 nm and a broad maxima around 570 nm. A comparison of this spectrum with that measured in the $N_3^{\bullet}$ radical reaction shows that the two peaks are red-shifted. Such behavior was reported[8b] earlier in the case of 5,6-dimethoxyindole. On going to pH 7, the spectrum recorded at the same time (40 μs) exhibited a sharp peak at 315 nm and a weak peak at 540 nm with a shoulder at 420 nm and is identical to that measured at 35 μs in the earlier[6] work. This spectrum is mostly made up of the $^{\bullet}$OH radical adduct since the characteristic indolyl radical peak at 540 nm is weak.

The computed UV−vis spectrum for the indolyl radical shows the maxima at 313 and 460 nm in vacuum and the latter is slightly red-shifted to 471 nm in water. The maximum at the lower wavelength is in accord with the experimental value (315−330 nm), but the longer wavelength value differs (Figure 1S in Supporting Information).

HTpe. The spectra recorded at 10 μs after the pulse in the $^{\bullet}$OH radical reaction with 1×10^{-3} mol dm^{-3} HTpe at pH 5 exhibited peaks at 375 and 420 nm and the decrease in absorption at lower wavelength with corresponding increase at 420 nm was seen on going to 200 μs (Figure 2). However, the spectra measured in neutral and basic media did not show any such transformation and the usual bimolecular decay was seen at the two wavelengths.

Energetics and Reactivity Parameters of (HTpe−OH)$^{\bullet}$ and (Tpe−OH)$^{\bullet}$ Adducts. The $^{\bullet}$OH radical is electrophilic in nature,[34] and its reactivity is structure dependent. Therefore, DFT calculations to examine the selectivity of its attack on HTpe and Tpe are interesting and the energetics of the $^{\bullet}$OH addition and the water elimination for the $^{\bullet}$OH adducts of both systems were determined using B3LYP/6-31+G(d,p) level of theory. Such calculations[35] on the relative stabilities for a number of $^{\bullet}$OH adducts of pyrimidines and purines were recently carried out. The thermodynamic parameters calculated for reactions 1 and 2 (Scheme 1) are tabulated in Table 1 in the case of HTpe.

It can be seen that the overall enthalpy of reactions 1 and 2 for (C2−OH)$^{\bullet}$ adduct is exothermic with $\Delta H_0 = -37.1$ kcal mol^{-1} and $\Delta G = -38.2$ kcal mol^{-1}. The first step, namely, $^{\bullet}$OH radical addition to HTpe, seems to depend strongly on the site of reaction. For example, the more energetically favorable positions were calculated to be 2 and 4. The two competing effects that dominate the reaction[36−38] are the frontier orbital π-electron density and the atomic Mulliken charge. However, no correlation of relative stabilities (ΔE_0) of different $^{\bullet}$OH radical adducts was found with Mulliken charge distribution in HTpe.

The distribution of unpaired electron spin density in the indoloxyl radical is shown in Figure 3 along with the π-electron density distribution from highest occupied molecular orbitals HOMO and HOMO-1 of the singlet ground state. According to chemical reactivity theory of Klopman and Salem,[36−38] the reaction proceeds in a way to produce the most favorable interaction energy, which is controlled by two factors: an

TABLE 1: Calculated Reaction Parameters of Different (HTpe−OH)• Adducts: Relative Stability ΔE_0, Reaction Enthalpy ΔH_0 and Gibbs Free Energy ΔG in kcal mol^{-1} for Reactions 1 and 2 (Scheme 1) after Zero Point Energy Correction

	ΔE_0	$\Delta H_0(1)$	$\Delta G(1)$	$\Delta H_0(2)$	$\Delta G(2)$
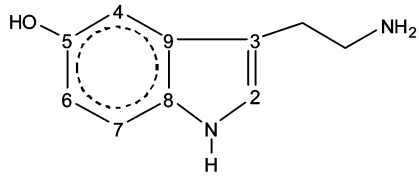					
C2-OH	0.0	-27.3	-18.0	-9.8	-20.2
C3-OH	+11.5	-26.5	-7.2	-20.0	-29.4
C4-OH	+2.3	-26.0	-15.2	-13.1	-23.0
C5-OH	+8.7	-18.6	-8.9	-18.5	-28.9
C6-OH	+9.2	-18.1	-8.9	-19.0	-29.3
C7-OH	+9.3	-18.1	-9.1	-19.0	-29.1
C8-OH	+17.1	-10.2	-0.5	-26.9	-37.7
C9-OH	+25.9	-1.4	+8.3	-35.7	-46.5

electrostatic interaction approximated by atomic charges and a frontier orbital interaction.

The electron distribution from highest occupied molecular orbitals HOMO and HOMO-1, which are close in energy (Figure 3A), shows that the most reactive places of HTpe ground state molecule are C_2, C_4, and C_6 with the largest electron density and C_4 and O in the case of the HTpe radical (Figure 3B).

Thus, in the case of HTpe, the •OH radical addition reaction is, apparently, governed by the high π-electron density at C4 from HOMO leading to the preferred formation of the (C4−OH)• adduct. The •OH radical addition at C2 should be also considered because of high π-electron density on C2 in HOMO-1, which are close in energy (0.2 eV) with HOMO. Further, due to the favorable geometry, the water elimination from the (C4−OH)• adduct is likely to proceed faster.

Similar calculations done for (Tpe−OH)• adducts have shown that the (C2−OH)• adduct is the only stable addition product in comparison to back reaction to the reactants which subsequently eliminates water to give the indolyl radical. The overall process was found to be exothermic with $\Delta H_0 = -27.3$ kcal mol^{-1} and $\Delta G = -27.9$ kcal mol^{-1} for reactions 1 and 2.

NO_2• and Br_2•− Radical Reactions with HTpe. The rates of reaction of NO_2• radical with HTpe were measured in neutral solutions where HTpe is in the protonated form and $k \sim 1 \times 10^7$ dm^3 mol^{-1} s^{-1} was determined. No reactivity of NO_2• radical with (1×10^{-3} mol dm^{-3}) Tpe was noticed. The second-order rate constant for the reaction of Br_2•− with HTpe evaluated from the linear plot (inset d of Figure 4) in neutral solution is near diffusion-controlled with $k = (3.7 \pm 0.1) \times 10^9$ dm^3 mol^{-1} s^{-1}. The lower reactivity of NO_2• radical is due to its lower reduction potential than that of Br_2•− radical.

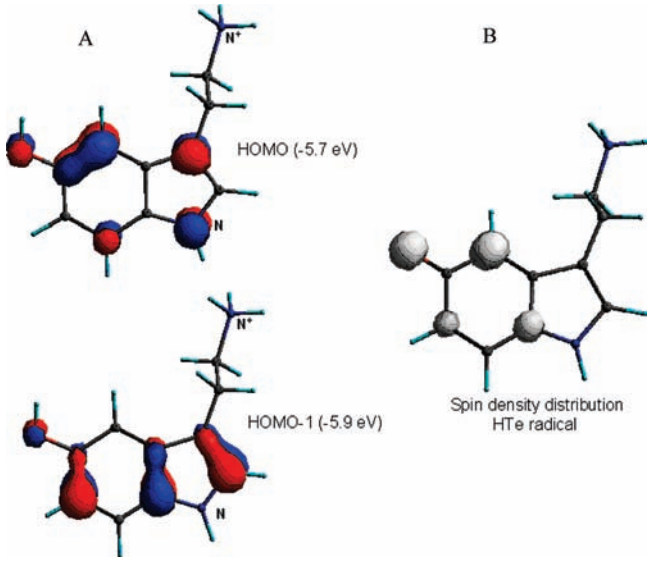

Figure 3. (A) Electron density distribution from HOMO and HOMO-1 of HTpe singlet ground state and (B) Distribution of unpaired electron spin density in HTpe radical.

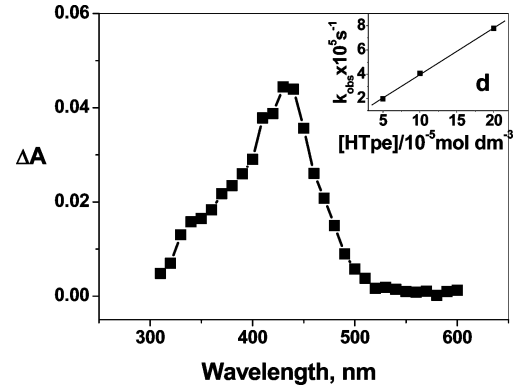

Figure 4. Transient absorption spectra obtained in reaction of Br_2•− radical with N_2O saturated solution of HTpe (1×10^{-3} mol dm^{-3}) at 10 μs after pulse (pH 7). Dose per pulse = 11.7 Gy. Inset (d) shows the linear plot of k_{obs} measured as a function of [HTpe] at 420 nm.

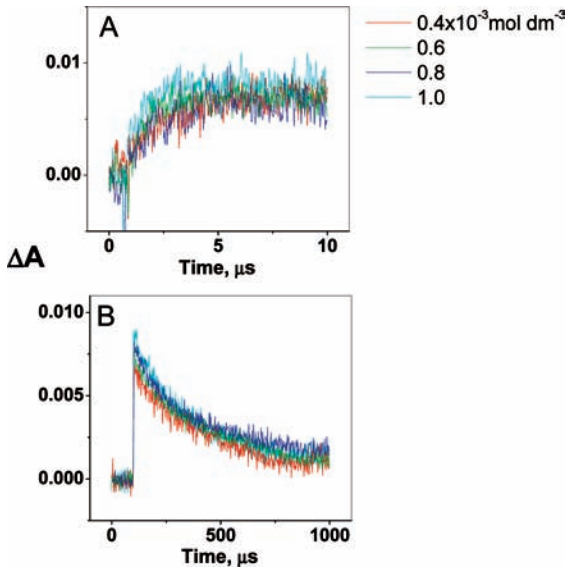

Figure 5. The absorption growth (A) and decay (B) at 530 nm generated by the pulse radiolysis of N_2O saturated aqueous solutions containing different concentrations of Tpe and 0.05 mol dm^{-3} NaN_3 at pH 7. Dose per pulse = 9 Gy.

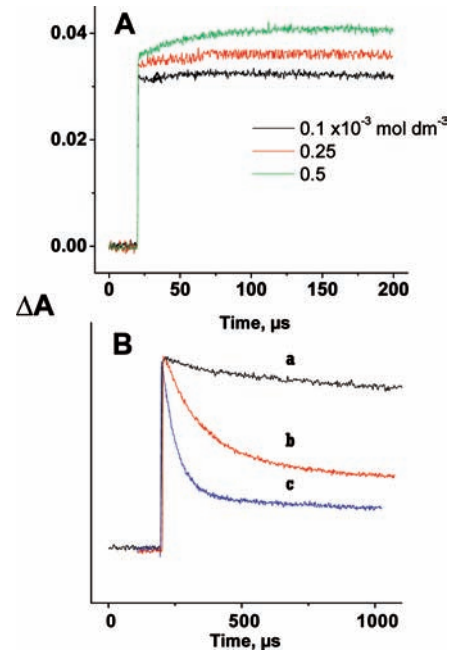

Figure 6. (A) Buildup of radical adduct measured at 420 nm in the reaction of $Br_2^{\bullet-}$ with HTpe ((0.1−0.5) × 10^{-3} mol dm^{-3}) at pH 9. (B) Decay of indoloxyl radical in the presence of (a) 0, (b) 50 × 10^{-6}, and (c) 100 × 10^{-6} mol dm^{-3} of ascorbate at pH 7. Dose per pulse = 9 Gy.

The absorption spectra in the reaction of $Br_2^{\bullet-}$ radical were recorded in the range 300−600 nm and the spectrum obtained with HTpe at pH 7 shown in Figure 4 exhibited a peak at 420 nm, which is attributed to the formation of the indoloxyl radical produced within 10 μs by the one-electron oxidation followed by deprotonation at the OH group.[14] Considering G ($Br_2^{\bullet-}$) = 6.9 per 100 eV at 0.1 mol dm^{-3} Br^- concentration in N_2O saturated solutions, based on the work of Schuler et al.,[39] the molar absorptivity at 420 nm was determined to be 5900 dm^3 mol^{-1} cm^{-1}. In contrast to the behavior observed with $Br_2^{\bullet-}$ radical, the absorption intensity at 420 nm measured in the $NO_2^{\bullet}$ radical reaction is lower which may be due to the escape of $NO_2^{\bullet}$ radical via reactions 4 and 5.

Excited-state calculations were done for the indoloxyl radical, and its calculated spectrum exhibited strong absorption at 370 nm and a shoulder at 330 nm in the gas phase. In contrast to the behavior observed with the indolyl radical, the solvent seems to have a profound effect on the indoloxyl radical spectrum in solution with three bands at 340, 380, and 407 nm and the value in the visible range is in good agreement with the experimentally measured maximum at 420 nm.

Radical Adduct Formation. In order to examine the radical adduct formation in the case of the indolyl radical, traces were recorded for different concentrations in the reaction of Tpe with $N_3^{\bullet}$ radical at pH 7 and Figure 5A depicts the growth of absorption (530 nm) at 10 μs where the intensities did not show any marked increase when the [Tpe] was increased from (0.4 to 1.0) × 10^{-3} mol dm^{-3} and only the usual bimolecular decay was seen on 1 ms (Figure 5B) suggesting lack of addition.

In contrast, in oxidation by $Br_2^{\bullet-}$ radical, an increase in intensities with rising concentration clearly indicating significant addition of indoloxyl radical to HTpe was seen as is evident from the absorption traces recorded at 420 nm in the range (0.1 to 0.5) × 10^{-3} mol dm^{-3} (Figure 6A) and its decay recorded on 1 ms (Figure 6B, trace a) shows marginal decrease. Further, the first half-life of bimolecular decay for [radical adduct] = 6 × 10^{-6} mol dm^{-3} was estimated to be 10 ms (not shown).

The association constant (K) for the radical adduct formation in the $Br_2^{\bullet-}$ reaction from the traces shown in Figure 6A for [HTpe] = (0.1−0.5) × 10^{-3} mol dm^{-3} was estimated to be (4.2 ± 0.5) × 10^4 dm^3 mol^{-1}. Similar behavior was also seen in the $^{\bullet}OH$ radical reaction where the association constant for [HTpe] = (0.05−1.0) × 10^{-3} mol dm^{-3} was determined to be (4.9 ± 0.2) × 10^4 dm^3 mol^{-1}. Since the concentration range is limited in the former reaction, the error in the measured value is larger. However, in the case of $NO_2^{\bullet}$ radical, the association constant was estimated to be 2.4 × 10^3 dm^3 mol^{-1}, which is an order of magnitude lower than that observed in the above two reactions indicating that relatively higher solute concentrations are needed for the addition to occur.

Reaction Pathways. All possible structures of the radical adduct formed from the interaction of the indoloxyl radical with both protonated and deprotonated forms of HTpe were considered for optimization. No significant differences were seen in the reaction enthalpies calculated for protonated and deprotonated forms of HTpe. But the values calculated for the protonated form were found to be sensitive when the solvent effect was applied and, therefore, only data obtained with the deprotonated form after applying solvent correction are discussed further.

Among the possible structures of the radical adduct that could be optimized from the interaction at C4′ and O′ positions of indoloxyl radical with C2, C4, and C6 of HTpe, only the structures (reactions 1−3) bonded through the C4′ of the indoloxyl radical due to the high-spin density (Figure 3) and the one formed through the H−O bond (reaction 4) are given in Scheme 2. The C−O bonded radical adducts are excluded because their subsequent reactions leading to the formation of stable dimer products, unlike in the case of C−C bonded structures, were not noticed.

All the C−C bonded structures of radical adduct were found to be endothermic in the gas phase. When the solvent effect was taken into account (optimized geometries in the gas phase and in water), the endothermicity was reduced in water. However, an energetically favorable exothermic structure formed through the H−O bond (Scheme 2) was obtained with a reaction

SCHEME 2: Structures of Possible C−C and H−O Bonded Radical Adducts Formed from Interaction of Indoloxyl Radical with HTpe and the Corresponding Reaction Enthalpies

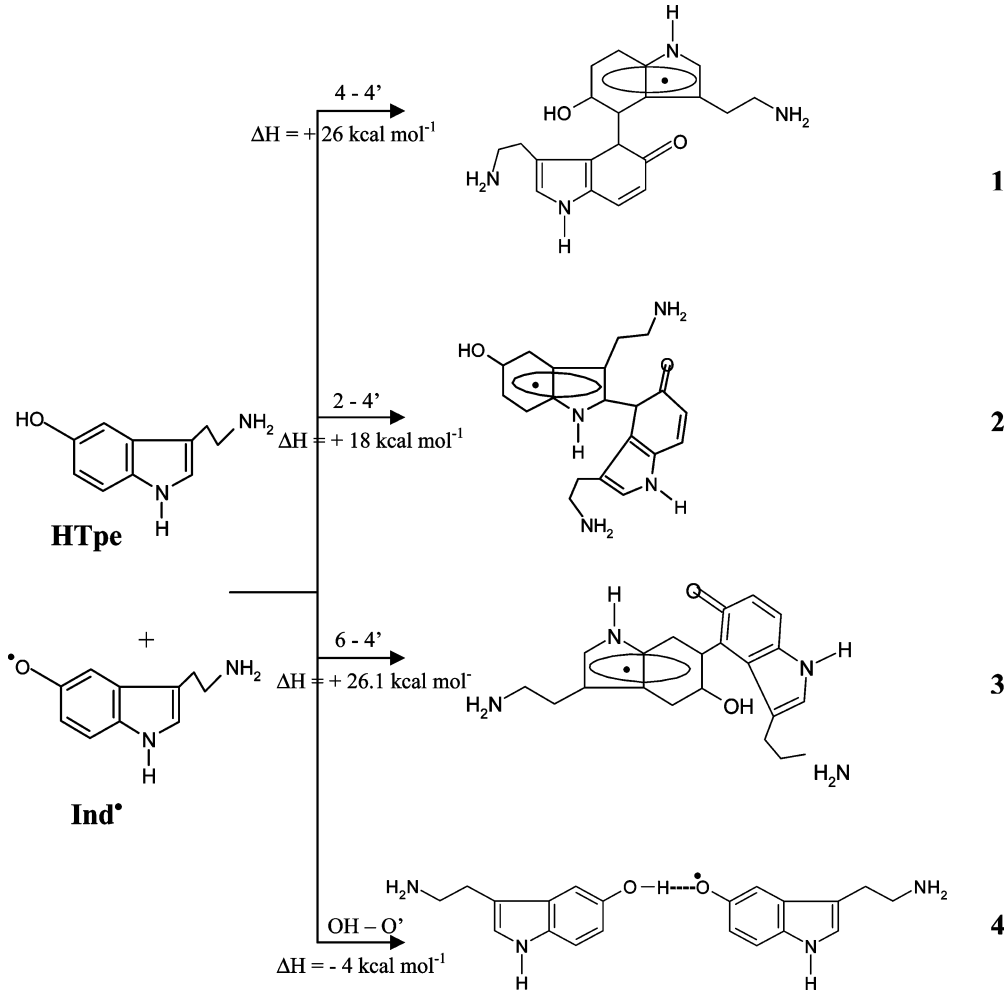

enthalpy of formation $\Delta H = -4$ kcal mol^{-1} and bond length 0.1819 nm. It should be noted that due to uncertainty in the calculations of hydrogen bonded systems in water, the estimated values may not be accurate. The H−O bonded radical adduct does not lead directly to C−C dimer products, but because of its exothermicity, it helps in the approach of the two reactants (indoloxyl radical and HTpe) with subsequent C−C radical adduct formation.

Similar to the indoloxyl radical, excited state calculations for the H−O bonded radical adduct (structure 4, Scheme 2) in the gas phase have shown the absorption maximum at 382 nm, but the solvent correction could not be applied. The calculation of its excitation energies in water (dielectric continuum model) was unsuccessful because of the convergence problem caused apparently by its large size, but it is expected to have the same spectral features as that of indoloxyl radical in water because of similar distribution of unpaired spin in both.

Calculations were extended to the formation of stable dimer products from the three corresponding C−C radical adducts and the sequence of reaction channels beginning from the interaction of indoloxyl radical with HTpe to the final formation of C4−C4′ dimer product, as an example, is depicted in detail in Scheme 3.

The C4−C4′ bonded radical adduct (structure 1, Scheme 2) undergoes disproportionation between two adducts to give products **b** and **c** (Scheme 3). Subsequently, compound **c** rearomatizes by intramolecular H shift to give finally the C4−C4′ dimer **d**. The overall reaction enthalpy for the whole process is exothermic with $\Delta H = -39$ kcal mol.$^{-1}$ Accordingly, ΔH values calculated for other two C2−C4′ (dimer **a**, Figure 2S in Supporting Information), C6−C4′ (dimer **b**) dimers are −44 and −21 kcal mol^{-1}, respectively.

Due to lack of (HTpe−Ind)$^{\bullet}$ radical adduct formation for low serotonin concentrations ($\leq$50 μM), the stable dimer products are formed by direct recombination of indoloxyl radical and the reaction enthalpies determined for the two C4−C4′ and C2−C4′ dimer products are −35 and −40 kcal mol^{-1}, respectively. It can be seen that the magnitude of reaction enthalpies in both cases, i.e., through radical adduct formation or direct dimerization of indoloxyl radical, does not significantly differ.

Our calculations were also extended to Tpe at the same B3LYP/6-31+G(d,p) level. According to the spin density distribution, the reactive sites of indolyl radical were found to be C3 and N1 and from the π-electron density distribution in HOMO, the reactive place of the Tpe ground state molecule was determined to be C_2. Of the several structures optimized for the radical adduct from the interaction of the indolyl radical with deprotonated Tpe, only the C2−N1′ structure was found to be exothermic $\Delta H = -4$ kcal mol^{-1} (Figure 3S in Supporting information). However, ΔG turned out to be positive with +10 kcal mol^{-1} indicating low probability of its formation in accord with the lack of radical adduct formation with Tpe observed in our pulse radiolysis experiments. However, the recombination of indolyl radicals leading to N−N bonded dimer product is

SCHEME 3: Reaction Pathways of C4−C4′ Radical Adduct a by Disproportionation and H Shift (Reaction 1) and by $K_3Fe(CN)_6$ Oxidation/Deprotonation (Reaction 2) Leading to Corresponding Stable Dimer Product d

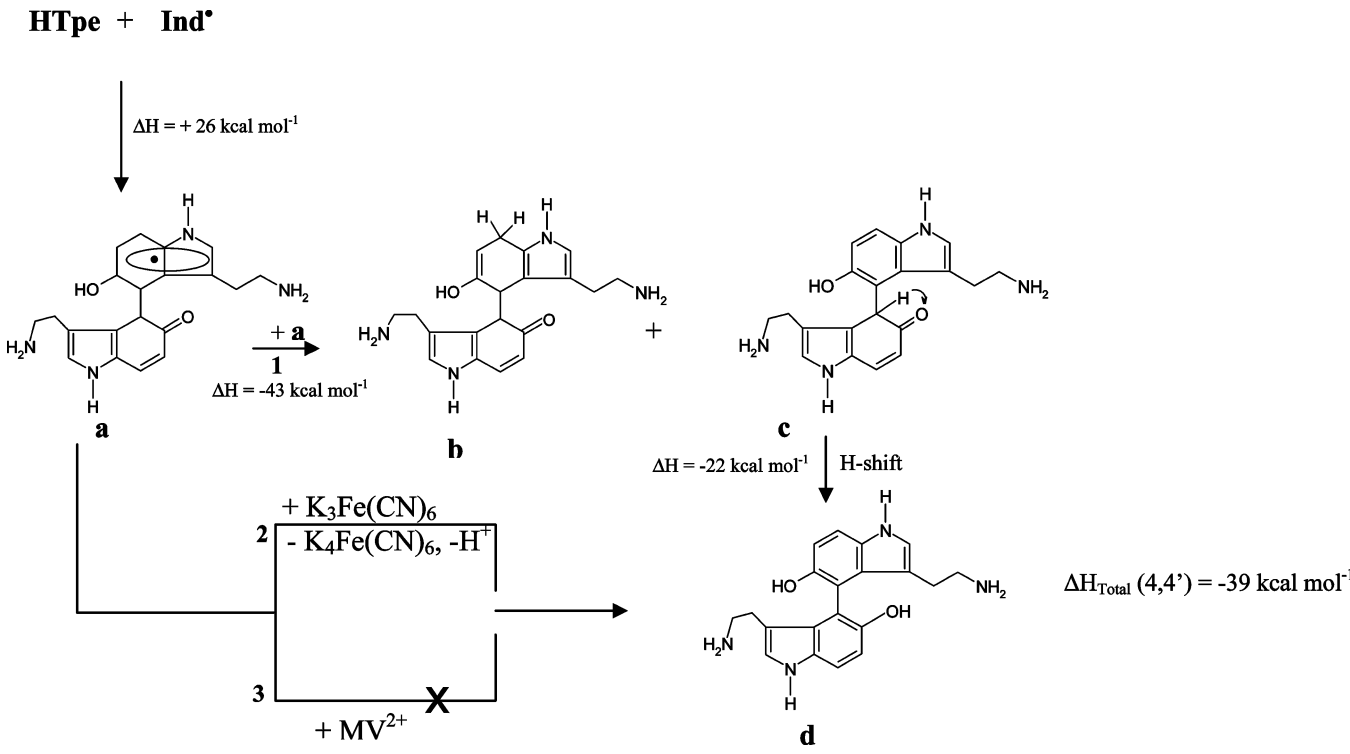

exothermic with ΔH and ΔG being −34 and −19 kcal mol^{-1} and the sequence of reaction pathways for formation of radical adduct by reaction of indolyl radical with Tpe molecule and stable dimer product by its direct recombination is shown in Figure 4S in the Supporting Information.

Product Analysis. The product analysis was performed by HPLC under steady-state radiolysis conditions for high (1×10^{-3} mol dm^{-3}, chromatograms A−D) and low (5×10^{-5} mol dm^{-3}, chromatogram E) HTpe concentrations and relevant chromatograms are shown in Figure 7. In the former case, experiments were conducted with (chromatograms A and C) and without (chromatograms B and D) 0.3×10^{-3} mol dm^{-3} $K_3Fe(CN)_6$. The formation of a single product with protocol 1 (chromatograms C and D) and an additional product using protocol 2 was formed during the first 35 min (chromatograms A, B, and E) and no further products were seen up to 60 min. On the basis of retention times in their work, the two products **2** and **3** formed using the protocol 2 are identified as C4−C4′ and C2−C4′ dimers (chromatograms A and B), respectively. The product eluted in protocol 1 is assigned to the symmetric dimer **2** (chromatograms C and D) which is expected to be the major product.

The detailed reaction sequence only for the C4−C4′ product formed with and without ferricyanide is shown in Scheme 3, since the same mechanism is operative for the C2−C4′ product. In the absence of ferricyanide, the dimer **d** is formed in a bimolecular reaction (reaction 1, Scheme 3) as discussed above from the H abstraction−H shift pathways by 2:1 stoichiometry. In contrast, in the presence of ferricyanide, the reaction proceeds by oxidation followed by deprotonation with 1:1 stiochiometry (reaction 2) by doubling its yield. This is evident from the observed peak areas for dimer **d** (product **2**) in chromatograms A and B where the absorbed dose (240 Gy) in the former is lower by 4-fold. A similar trend was also observed in chromatograms C and D using the other protocol. Considering $G(Br_2^{\bullet-}) = 6.9$ per 100 eV and assuming that the intermediate radicals are entirely converted into the two isomeric C4−C4′ and C2−C4′ dimers and their molar extinction coefficients are comparable, their yields are estimated to be G(C4−C4′) = 4.1 and G(C2−C4′) = 2.8. Though the C2−C4′ dimer product is thermodynamically more stable by 5 kcal mol^{-1}, the lesser HOMO-1 energy and weaker overlap of orbitals result in its lower yield. On the other hand, the formation of C4−C4′ dimer is kinetically more favored due to the large electron spin density on C4 position of both the reactants.

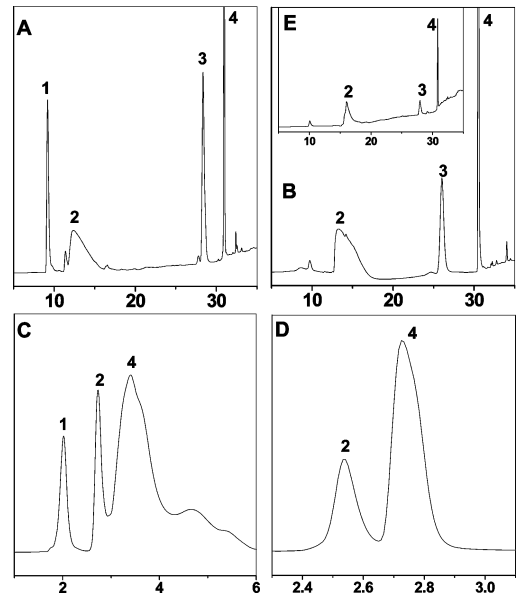

Figure 7. HPLC chromatograms obtained on irradiation of 1×10^{-3} mol dm^{-3} HTpe at pH 7 in the presence (A and C) and absence (B and D) of 0.3×10^{-3} mol dm^{-3} $K_3Fe(CN)_6$ and 5×10^{-5} mol dm^{-3} HTpe (E). Protocol 1 (C and D) and protocol 2 (A, B, and E) and dose 240 (A and C) and 1000 Gy (B, D and E). Products: (1) $K_3Fe(CN)_6$, (2) C4−C4′ dimer, (3) C2−C4′ dimer, and (4) HTpe.

SCHEME 4: Dimerization Reaction Pathway of Indoloxyl Radical a Resulting into C4−C4′ (b) and C2−C4′ (c) Stable Dimers (Reaction 1) and Its Redox Reaction with $ABTS^{2-}$ and Ascorbate (Reactions 2 and 3)

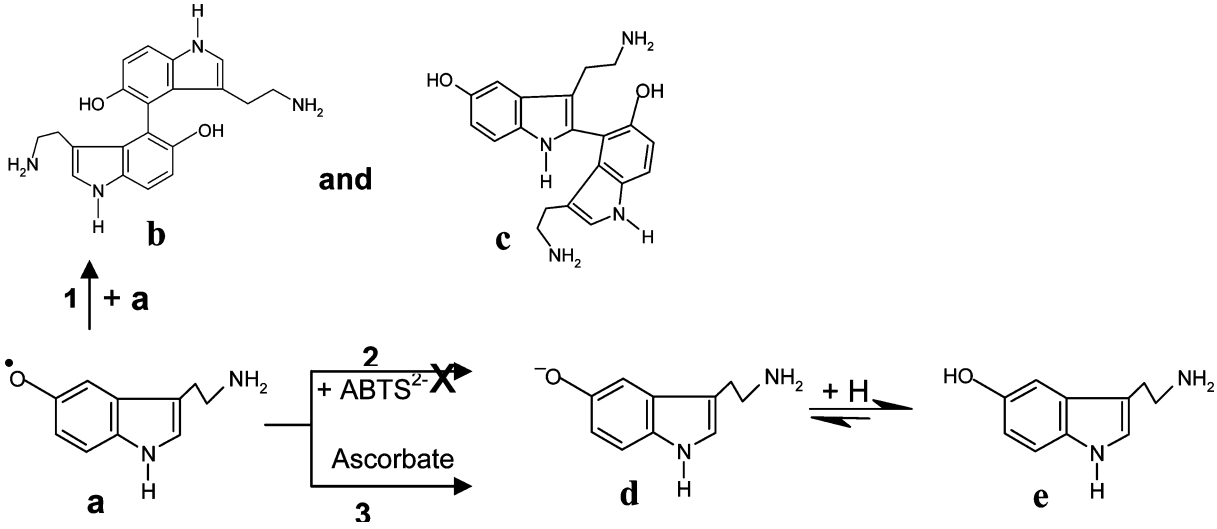

In the case of low HTpe concentration, the direct coupling of the indoloxyl radical gives C4−C4′ and C2−C4′ stable dimers (products 2 and 3, chromatogram 7E), and the sequence of reactions showing their formation (products b and c) is shown in reaction 1, Scheme 4.

The redox properties of the indoloxyl radical formed were studied using the reductants, $ABTS^{2-}$ and ascorbate with reduction potentials 0.63 and 0.3 V, respectively. Less than 20% of 6×10^{-6} mol dm^{-3} indoloxyl radical produced on radiolysis was scavenged by 6×10^{-5} mol dm^{-3} $ABTS^{2-}$ (reaction 2, Scheme 4). The remaining underwent, in competition, radical adduct formation. On the other hand, under similar conditions, about 75% of the indoloxyl radical was repaired by ascorbate (reaction 3, Scheme 4 and Figure 6B, traces b and c) consistent with its reduction potential.

Similarly, the oxidation of the intermediate radical adducts was tested using MV^{2+}, but the yield of $MV^{\bullet+}$ was found to be negligible (reaction 3, Scheme 3) suggesting that these radical adducts require a stronger oxidant such as ferricyanide as found in our product analysis (reaction 2, Scheme 3).

Conclusions

Radiation-induced oxidation of Tpe and HTpe by $^{\bullet}OH$, $N_3^{\bullet}$, and $Br_2^{\bullet-}$ radicals was carried out by pulse radiolysis and analyzed by DFT calculations. All the rate constants measured in this work are nearly diffusion-controlled. Even the weakly oxidizing $NO_2^{\bullet}$ radical was found to oxidize serotonin ($k \sim 1 \times 10^7$ dm^3 mol^{-1} s^{-1}) to give the indoloxyl radical. The indoloxyl radical undergoes addition to HTpe resulting in the formation of radical adducts for concentrations usually encountered in living organisms (>1×10^{-3} mol dm^{-3}) and the lifetimes of these radical adducts were found to be tens of milliseconds. The addition step was found to be endothermic with a barrier of 18−26 kcal mol^{-1} and is rate determining because the subsequent sequence of reactions leading to neurotoxic stable dihydroxy C−C dimer[4] products is exothermic. A significant finding of our theoretical calculations is that the formation of lethal dimer products both by (HTpe−$Ind^{\bullet}$ radical adduct H abstraction−H shift) reaction and direct recombination of indoloxyl radical are equally efficient thermodynamic processes that could interfere with the normal metabolic pathways. The repair of the indoloxyl radical was observed to be effective only with a relatively stronger reductant such as ascorbate and, thus, any defect in the serotonin metabolism will lead to the formation of toxic dimer products. In contrast, such adduct formation of the indolyl radical with Tpe was not noticed with ΔG being positive. The salient feature of this work is that the indolyl radical is less reactive with tryptamine but it is far more reactive with itself than is the indoloxyl radical. Quantum chemical calculations complemented our pulse radiolysis data in the understanding of the reaction mechanism and determination of relative stabilities of HTpe−OH adducts toward the formation of indoloxyl radical by dehydration.

Acknowledgment. The authors wish to thank DAE for supporting the LINAC facility and Dr. A. S. Kumbhar for extending its use. B.S.M.R. would like to thank the DAE-BRNS for the award of the Raja Ramanna Fellowship and P. Gaikwad is thankful to the BARC for financial support under the BARC−PU Collaborative Research Program.

Supporting Information Available: Calculated UV−visible spectra of indoloxyl and indolyl radicals in vacuum and water (Figure 1S), energetics for formation of C2−C4′ and C6−C4′ bonded dimer products (Figure 2S), electron density distribution from HOMO of Tpe singlet ground state, spin density in Tpe radical and optimized structure of exothermic C2−N1′dimer radical (Figure 3S), and energetics for formation of radical adduct by reaction of indolyl radical with Tpe and stable dimer product by its direct recombination (Figure 4S). This material is available free of charge via Internet at http://pubs.acs.org.

References and Notes

(1) Shen, X.; Lind, J.; Merenyi, G. *J. Phys. Chem.* **1987**, *91*, 4403.
(2) Herraiz, T.; Galisteo, J. *Free Radical Res.* **2004**, *38*, 323.
(3) Wrona, M. Z.; Dryhurst, G. *Chem. Res. Toxicol.* **1998**, *11*, 639.
(4) Dryhurst, G. *Chem. Rev.* **1990**, *90*, 795.
(5) Jovanovic, S. V.; Steenken, S.; Simic, M. G. *J. Phys. Chem.* **1990**, *94*, 3583.
(6) Hela, P. G.; Anipindi, N. R.; Priyadarsini, K. I.; O' Neill, P. *J. Phys. Chem. B* **1999**, *103*, 8606.
(7) Candeias, L. P.; Wardman, P.; Mason, R. P. *Biophys. Chem.* **1999**, *67*, 229.
(8) (a) Al-Kazwini, A. T.; O'Neill, P.; Adams, G. E.; Cundall, R. B.; Junino, A.; Maignan, J. *J. Chem. Soc., Perkin Trans.* **1992**, *2*., 657. (b) Al-Kazwini, A. T.; O'Neill, P.; Adams, G. E.; Cundall, R. B.; Jacquet, B.; Lang, G.; Junino, A. *J. Phys. Chem.* **1990**, *94*, 6666.

(9) Lambert, C.; Land, E. J.; Riley, P. A.; Truscott, T. G. *Biochim. Biophys. Acta* **1990**, *1035*, 319.
(10) Al-Kazwini, A. T.; O'Neill, P.; Adams, G. E.; Cundall, R. B.; Maignan, J.; Junino, A. *Melanoma Res.* **1994**, *4*, 343.
(11) Naik, G. H.; Priyadarsini, K. I.; Mohan, H. *Phys. Chem. Chem. Phys.* **2002**, *4*, 5872.
(12) Blanchard, B.; Dendane, M.; Gallard, J. F.; Houee-Levin, C.; Karim, A.; Payen, D.; Launay, J. M.; Ducrocq, C *Nitric Oxide* **1997**, *1*, 442.
(13) Naik, G. H.; Priyadarsini, K. I.; Mohan, H. *Res. Chem. Intermed.* **2003**, *29*, 641.
(14) Naik, G. H.; Priyadarsini, K. I.; Maity, D. K.; Mohan, H. *J. Phys. Chem. A* **2005**, *109*, 2062.
(15) Goldstein, S.; Merenyi, G.; Russo, A.; Samuni, A. *J. Am. Chem. Soc.* **2003**, *125*, 8364.
(16) Ford, E.; Hughes, M. N.; Wardman, P. *Free Radical Biol. Med.* **2002**, *32*, 1314.
(17) Huie, R. E. *Toxicolology* **1994**, *89*, 193.
(18) Yadav, P.; Kulkarni, M. S.; Shirdhonkar, M. B.; Rao, B. S. M. *Curr. Sci.* **2007**, *92*, 599.
(19) Gaikwad, P.; Priyadarsini, K. I.; Rao, B. S. M. *Radiat. Phys. Chem.* **2008**, *77*, 1124.
(20) Buxton, G. V.; Stuart, C. R. *J. Chem. Soc., Faraday Trans.* **1995**, *91*, 279.
(21) Grätzel, M.; Henglein, A.; Lilie, J.; Beck, G. *Phys. Chem.* **1969**, *73*, 646.
(22) Broszkiewicz, R. K. *Bull. Acad. Pol. Sci., Ser. Sci. Chim.* **1976**, *24*, 221.
(23) Schwartz, S. E.; White, W. H. *Adv. Environ. Sci. Technol.* **1983**, *12*, 1.
(24) Augusto, O.; Bonini, M. G.; Amanso, A. M.; Linares, E.; Santos, C. C. X.; Menezes, S. L. De. *Free Radical Biol. Med.* **2002**, *32*, 841.
(25) Wrona, M. Z.; Dryhurst, G. *J. Org. Chem.* **1987**, *52*, 2817.
(26) Wrona, M. Z.; Dryhurst, G. *J. Org. Chem.* **1989**, *54*, 2718.
(27) Becke, A. D. *J. Chem. Phys.* **1993**, *98*, 5648.
(28) Becke, A. D. *J. Chem. Phys.* **1996**, *104*, 1040.
(29) Lee, C. T.; Yang, W. T.; Parr, R. G. *Phys. Rev. B* **1988**, *37*, 785.
(30) NY Jaguar 7.0, Schrodinger LLC, New York, 2008.
(31) Tannor, D. J. M.; Murphy, B.; Friesner, R.; Sitkoff, R. A.; Nicholls, D.; Ringnalda, A.; Goddard, W. A. M.; Honig, B *J. Am. Chem. Soc.* **1994**, *116*, 11875.
(32) Bauernschmitt, R.; Ahlrichs, R. *Chem. Phys. Lett.* **1996**, *256*, 454.
(33) Frisch, M. J.; Trucks, G. W.; Schlegel, H. B.; Scuseria, G. E.; Robb, M. A.; Cheeseman, J. R.; Montgomery, J. A., Jr.; Vreven, T.; Kudin, K. N.; Burant, J. C.; Millam, J. M.; Iyengar, S. S.; Tomasi, J.; Barone, V.; Mennucci, B.; Cossi, M.; Scalmani, G.; Rega, N.; Petersson, G. A.; Nakatsuji, H.; Hada, M.; Ehara, M.; Toyota, K.; Fukuda, R.; Hasegawa, J.; Ishida, M.; Nakajima, T.; Honda, Y.; Kitao, O.; Nakai, H.; Klene, M.; Li, X.; Knox, J. E.; Hratchian, H. P.; Cross, J. B.; Adamo, C.; Jaramillo, J.; Gomperts, R.; Stratmann, R. E.; Yazyev, O.; Austin, A. J.; Cammi, R.; Pomelli, C.; Ochterski, J. W.; Ayala, P. Y.; Morokuma, K.; Voth, G. A.; Salvador, P.; Dannenberg, J. J.; Zakrzewski, V. G.; Dapprich, S.; Daniels, A. D.; Strain, M. C.; Farkas, O.; Malick, D. K.; Rabuck, A. D.; Raghavachari, K.; Foresman, J. B.; Ortiz, J. V.; Cui, Q.; Baboul, A. G.; Clifford, S.; Cioslowski, J.; Stefanov, B. B.; Liu, G.; Liashenko, A.; Piskorz, P.; Komaromi, I.; Martin, R. L.; Fox, D. J.; Keith, T.; Al-Laham, M. A.; Peng, C. Y.; Nanayakkara, A.; Challacombe, M.; Gill, P. M. W.; Johnson, B.; Chen, W.; Wong, M. W.; Gonzalez, C.; and Pople, J. A.; *Gaussian 03*; Gaussian, Inc.:Pittsburgh, PA, 2003.
(34) Anbar, M.; Meyerstein, D.; Neta, P. *J. Phys. Chem.* **1966**, *70*, 2660.
(35) Naumov, S.; Sonntag, C. v *Radiat. Res.* **2008**, *169*, 353.
(36) Klopman, G. *J. Am. Chem. Soc.* **1968**, *90*, 223.
(37) Salem, L. *J. Am. Chem. Soc.* **1968**, *90*, 543.
(38) Fleming, I. *Frontier Orbitals and Organic Chemical Reactions*; Wiley: Chichester, 2002.
(39) Schuler, R. H.; Hartzell, A. L.; Behar, B. *J. Phys. Chem.* **1981**, *85*, 192.

JP901315Q